Published in final edited form as:
Anal Biochem. 2008 September 15; 380(2): 315–322. doi:10.1016/j.ab.2008.05.048.

Real-Time PCR Quantification Using A Variable Reaction Efficiency Model

Adrian E. Platts[1,2], **Graham D. Johnson**[2], **Amelia K. Linnemann**[1], and **Stephen A. Krawetz**[1,2,3]

1*Center for Molecular Medicine & Genetics*

2*Department of Obstetrics and Gynecology, Wayne State University School of Medicine*

3*Institute for Scientific Computing, MS ABIO-08-201*

Abstract

Quantitative real-time PCR remains a cornerstone technique in gene expression analysis and sequence characterization. Despite the importance of the approach to experimental biology the confident assignment of reaction efficiency to the early cycles of real-time PCR reactions remains problematic. Considerable noise may be generated where few cycles in the amplification are available to estimate peak efficiency. An alternate approach that uses data from beyond the log-linear amplification phase is explored with the aim of reducing noise and adding confidence to efficiency estimates. PCR reaction efficiency is regressed to estimate the per-cycle profile of an asymptotically departed peak efficiency, even when this is not closely approximated in the measurable cycles. The process can be repeated over replicates to develop a robust estimate of peak reaction efficiency. This leads to an estimate of the maximum reaction efficiency that may be considered primer-design specific. Using a series of biological scenarios we demonstrate that this approach can provide an accurate estimate of initial template concentration.

Keywords

PCR; quantification; efficiency; NLM; transcription

Introduction

The quantitative real-time Polymerase Chain Reaction [1] is perhaps the most well established technique used for high resolution DNA, and indirectly, RNA, quantification. While alternative and massively parallel assays are increasingly available, PCR has remained the technology of choice for validating high-throughput data [2]. PCR sensitivity ranges from only a few amplicons through fully 6 orders of magnitude typically with a replicate covariance of less than 2% [3], making developments to PCR quantification of considerable significance for biological research.

Correspondence to: Stephen A. Krawetz, Charlotte B. Failing Professor of Fetal Therapy and Diagnosis, 253 C.S. Mott Center; 275 East Hancock; Detroit, MI, USA 48201, **Laboratory phone:** 313-577-0765; **Office phone:** 313-577-6770; FAX: 313-577-8554, **Email:** steve@compbio.med.wayne.edu.

Comprehensive reviews of the protocols, primer selection criteria and biophysical constraints necessary in designing a real-time PCR experiment are available (www.gene-quantification.de) [4;5;6;7]. Once design choices have been made and measurements of a multi-cycle PCR amplification process acquired, initial template quantification is required. The fractional number of cycles (C) required to generate a fluorescent signal exceeding an arbitrary threshold (t) is generally assessed. From this value a cycle-zero fluorescence that is proportionate to the concentration of the initial DNA template sequence is inferred. Each additional cycle required to achieve C_t approximately halves the initial fluorescence estimate relative to the threshold t. Consequently, a change in value of C_t between any two amplification processes suggests the relative difference in initial templates from a baseline to an experimental condition. In an ideal reaction the value $2^{C_1}/2^{C_2}$, i.e. $2^{(C_1 - C_2)}$, yields the ratio difference in initial templates arising from the shift in C_t between cycles C_1 and C_2.

However PCR rarely proceeds as such an ideal reaction. Even small differences in the amplification efficiencies of reactions will lead to detectable differences in C_t whether or not the concentrations of the starting templates differ. Approaches are available to adjust for some of the template-linked quality factors that may inhibit the progress of a reaction [8;9]. C_t values can be compared between both experimental states and controls such as ‘house-keeping’ genes or spike-in transcripts. Changes in control C_t values are combined with those between conditions ($2^{\Delta\Delta C_t}$) to describe differences in sample quality. The appropriateness of endogenous reference standards such as 18S rRNA, GAPDH and VEGF have come into question [10;11;12]. In addition, the readily visible portion of the reaction curve can be a poor indicator of where an appropriate (efficiency) matched control has been selected. Dilution strategies have been the most successfully explored to establish control and target gene efficiencies although these may require multiple replicate dilutions in order to establish efficiency with confidence [13].

Explicit corrections for differences between reaction kinetics have proven a difficult and sometimes unreliable alternative. Modifying exponential terms risks introducing substantial adjustment error [14]. However, if achieved, these approaches could describe reaction efficiency differences and reduce the impact of other confounding factors such as competition between parallel in-tube reactions and crosstalk between flours. Hence the development of efficiency corrected PCR approaches without the strict requirement for matched efficiency controls [15] continues to be desirable.

Several means to computationally correct for reaction efficiency have been described. Linearization of the exponential reaction through a log transformation allows fluorescence to be regressed back to its $zero_{th}$ cycle and continues to be the approach most widely adopted [9;16;17]. Reaction efficiencies below 100% yield shallower gradients in the log-transformed signal thereby generating proportionately larger starting template estimates. While useful, these approaches are limited by real-world considerations. Ideally, the log-linear phase of the amplification would be free of background noise, but it rarely is. At a very low signal, background effects such as CCD thermal noise and shot noise, lead to reduced reliability in the points from which the linear regression tangent is calculated. The log-linear phase may be significantly departed, only a few cycles beyond these high noise measurements, even as the signal to noise ratio improves. This can result in an estimate of the concentration of the initial template that is highly sensitive to the selection or exclusion of signal points. To offset this limitation an extended set of points can be included using more advanced ground-phase and sigmoid models [18] to approximate the development of the entire reaction and thereby indirectly estimate the relative exponential efficiencies between amplifications. These and other models have recently been reviewed [19].

Confounding many analytical assumptions, serial PCR reactions may only approximate and never truly sustain exponential progression [20]. The progress of a multi-cycle PCR amplification reaction is impeded by, (A), conditions that limit its maximum efficiency and (B) by processes that reduce the reaction efficiency on a per-cycle basis. Examples of type-A factors may include reagent quality, primer design, the impediment to amplification generated by secondary structure even at weak primer hairpins as well as other unique sub-features residing between the primers within the template. Examples of type-B constraints likely include the decreasing availability of reagents such as dNTPs for *de-novo* synthesis, and the ongoing degradation of the polymerase as the reactions progress. During the early cycles this steady reduction in efficiency from its maximum may be small. However, as the reaction proceeds and fluorescence becomes detectable, the effect of the continued reduction in efficiency and hence an imperfect log-linear progression generally becomes evident. Accordingly to reduce noise and increase the confidence when estimating efficiency an alternative approach that uses data from beyond the log-linear amplification phase was developed. PCR reaction efficiency is regressed to estimate the per-cycle profile of asymptotically departed peak efficiency, even when this is not closely approximated in the measurable cycles. This leads to an estimate of the maximum reaction efficiency that may be considered primer-design specific. The utility of this strategy is demonstrated in a series of scenarios described in this communication.

Methods

KLAB-PCR (**K**rawetz **LAB**oratory-**PCR** http://klab.med.wayne.edu/KLABPCR.zip) is a tool that implements two algorithms to quantify the starting template in a PCR reaction. The first is a modified C_t strategy that assumes an ideal efficiency and is calculated for reference. The second employs a parametric fitting approach to construct a non-linear approximation to the reaction efficiency that is regressed backwards to establish a peak efficiency. The implementation can use data from a single PCR reaction, or from several reactions where the same primers are used yielding a consensus of peak efficiency. We have tested these two approaches using standard dilution studies [21] to estimate the extent to which the efficiency was accurately determined and have adapted this approach as part of our routine PCR analysis. The results suggest that this non-linear model may represent a promising alternative to C_t that obviates the need for internal controls.

C_t Model

KLAB-PCR implements a refined C_t approach. The ideal reaction efficiency is assumed for all reactions. For each series, the subset of cycles over which an exponential development is most closely approximated over three cycles is identified. Evidence of product (T_n) at the central cycle is then taken as the cycle from which to assume $T_n = T_0 2^n$ and hence $T_0 = T_n/2^n$ While essentially the C_t approach, the threshold is independently calculated through the closest approximation to a low-noise exponential phase for each reaction, hence both cycle C and threshold t can vary.

Non-Linear Model

Extending work on exponential sigmoid approaches to reaction efficiency [20] we sought to explore alternate general biological models for the progressive deterioration of an exponential amplification. The model assumes that the amplification reaction has an inherent maximum efficiency that decreases at each cycle as reagents age and as competition for a reducing supply of resources increases for each amplicon. This generates the basic recursion relationship (Equation 1) for the amplification reaction. The multiple effects that serially reduce efficiency from a maximum (E_{max}) are represented by the compound function G. This function describes the aggregate impact of (k) confounding elements (Equation 2) that will ultimately fully quench

the reaction. Each of the k components of G at amplification cycle$_{i+1}$ is assumed to be generated by an independent function of T_i, the total template at the ith cycle of amplification.

$$T_{i+1}=T_i\,(E_{\max}-G\,(T_i)) \quad \text{(Eq. 1)}$$

$$G\,(T_i)=\sum_{n=1}^{k} g_n\,(T_i) \quad \text{(Eq. 2)}$$

Ideally, amplification E_{max} would be 2.0 (100% efficiency) and all components of G constant and zero. However, in most reactions, E_{max} will be less than 2.0, a type A constraint, and G always rises as the reaction progresses as a consequence of type-B constraints. When E_{max}-G (T_i) reaches 1, amplification is essentially terminated. The term E_{max}-G(T_i) is thus the effective reaction efficiency at the ith cycle, $E_{i(effective)}$. As expected (Figure 1A) even simple functions may serve to model G in ways that generally approximate the fluorescence trends observed during amplification. Clearly the reaction may rapidly depart from the maximum efficiency and become limited by G (Figure 1B). It is also evident that estimates of the log-linear gradient at later cycles increasingly underestimates the efficiencies of the earlier cycles (Figure 1C). By using a model of $E_{i(effective)}$ that is allowed to vary and is carried back to cycle zero, an estimate of the initial template that inherently recognizes a declining efficiency prior to observating the measurable fluorescent signal should be possible.

G is anticipated to be a higher-order function that will vary in form between reactions as the design and environment factors that contribute to the deterioration of an exponential reaction vary. It is the task of the algorithm to approximate a representative function G from the reliable signal data. To accomplish this, G is assumed to be a continuous non-periodic function (Equation 3), that can be closely approximated by a truncated series of power terms.

$$G\,(T_i)\approx\frac{1}{K_0}\sum_{j=1}^{10}K_j T_i^{n(j)},\mathrm{n\,(j)}:[0.2,0.4,\ldots,1.8,2.0] \quad \text{(Eq. 3)}$$

Values for the exponents $0\leq n>2$ were readily removed from consideration since they lead to non-physical models where runaway and cyclical amplification processes are respectively generated. Using a large test dataset generated primarily on MJ Research (BioRad) Chromo4, but also other systems including the ABI 7500, Corbett LifeSciences Rotor-Gene and Stratagene Mx3005, we estimated the weight for each exponent term in the set n(j). This was performed by serially adding terms to a model, minimizing the residual (Equation 4), and recording the weight K_j for each term. Given *x*, the cycle at which reliable signal is first detected, and *max*, the cycle at which the 95% maximum signal is attained, T(obs) and T(pred) are the observed signal and the predicted signal used to estimate a model residual. The higher-order terms should have a weak impact on the early cycles of a reaction but rapidly clamp the developing amplification, while low-order terms have an impact that is evident from the earliest cycles.

$$\mathrm{residual}=\sum_{i=x}^{\mathrm{Max}}\left|T(\mathrm{obs})_i-T(\mathrm{pred})_i\right|w_i \quad \text{(Eq. 4)}$$

While the different terms varied between systems it was readily apparent that weights for $J>5$ (ie $n(j)\geq 1.2$) became vanishingly small in most reactions due to the unrealistic rapid quenching of the reaction in these models. Similarly the contributions made by lower-order terms $j<2$ ($n(j)<0.2$) were also small reflecting the very protracted reaction duration that would be simulated. Hence only the weights K_j for $2\leq j\leq 5$ ($0.4\leq n\leq 1.0$) and E_{max} are estimated in the current implementation. Optimization of weights takes place again through residual minimization rather than differentiation as has been undertaken in other exponential models [18]. Contributions to the residual are not considered equal, but are adjusted (*w*) by cycle.

Following removal of any ground-state signal the weights are adjusted with earlier amplification cycles where signal/noise is close to zero, *w* is low, while cycles close to a log-linear phase contribute more, and finally the later cycles of amplification are assigned a decreasing weight as the reaction progresses through its log-linear phase to termination.

Implementation

The KLAB-PCR package was implemented in two parts to aid cluster-based parallelism for large projects. The user interface and scheduling were developed in object oriented VisualBasic (RealSoftware.com) while the core modeling ('child') elements were developed in C++ using Microsoft Visual Studio (2005).

The system allows the user to specify the total effective number of CPUs available. The scheduling component (Figure 2) then maintains a parallel number of child modeling instances using the operating system to distribute the processes over the available resources. The child model uses a two-stage approach to estimate the unknown variables in the power series. In the first stage an initial estimate of E_{max} is calculated by seeking the optimum fit from a series in which only the most significant power terms are modeled. These estimates are then averaged over any available replicates using a trimmed mean to develop a robust estimate of maximum efficiency. E_{max} is then fixed in the second iteration of modeling and the higher order power series elements are estimated while the lower order terms are optimized. Finally the scheduling application assesses the models provided by the child process and assigns a fit index to each ranging from zero, when no difference between model and experiment is observed, to higher values when increasing weaknesses in the models are evident. Weak models and curves that could not be modeled are flagged.

PCR

All PCR reactions were carried out in a 20 μL volume utilizing the Sigma SYBR® Green JumpStart™ Taq™ ReadyMix system and evaluated on the Chromo4 real time PCR detection system (Bio-Rad). All results were analyzed using the KLab-PCR program.

PCR validation of loop and nuclear matrix fractionated DNAs assessed by CGH (Comparative Genomic Hybridization) were carried out using 5 ng template DNA and a final primer concentration of 2 μM per reaction. Quantification of DNA was determined using PicoGreen™ (Molecular Probes) fluorometry [22]. Cycling conditions were 94°C for 2 min, followed by 45 cycles of 94°C for 30 s, 65°C for 1 min, and 72°C for 1 min (Table 1).

Reverse transcription of 5 μg of total testis RNA was performed using the Invitrogen Superscript III™ system. All PCR reactions contained 5 ng cDNA and a final primer concentration of 1 μM. Cycling conditions were 95°C for 15 min, followed by 45 cycles of 94°C for 20 s, 64°C for 1 min, and 72°C for 30 s (Table 1).

Zygosity was determined using a dilution series of 2.5, 5, and 10 ng of genomic DNA. All reactions had a final primer concentration of 1 μM. Reactions were carreid out for 35 cycles And were initiated at 95°C for 15 min, followed by 45 cycles of 94°C for 20 s, 64°C for 1 min, and 72°C for 30 s as summarized in Table 1.

Results and Discussion

The successful application of any algorithm is ultimately limited by the sensitivity and linearity of the measuring instrument. As illustrated in Figure 3, background noise generally obscures the signal from the fluorescently tagged product over many of the early amplification cycles. In estimating the form of the reaction curve the algorithms would be limited to the detectable signal available around cycle 26 and beyond. While the log-linear phase of the reaction appears

most consistent at cycle 26–27 (M1), it is apparent from the *increasing* efficiency data that these cycles are most likely compromised by poor measurement resolution and the non-linearity of the instrument at low signal.

To test the two approaches an intergenic chromosome 16 genomic template (Table 1) was serially diluted from an arbitrary starting concentration (10 units) to 5 and 2.5 units. These concentrations were plotted against the predictions of the two algorithms to estimate linearity and dilution accuracy. When the efficiency is correctly determined the dilution rate approaches 1. When the reaction efficiency is close to 100% both the C_t and non-linear models are concordant (Figure 4). In contrast, when the reaction efficiency falls significantly below 100%, the C_t approach while still predicting a linear dilution, over-estimates the dilution. Conversely, the non-linear model shows both high linearity and continues to reflect the experimental dilutions (Figure 5). With 'good data' the non-linear approach is generally robust. However, in those cases where the experimental data is subject to a high background it may not be possible to model the earlier development phase of the reaction. In this case the C_t method may provide a useful alternative when used with the standard comparators.

Validation of consistency of the algorithm with respect to multiple near-identical amplification reactions was demonstrated using a manufacturer supplied 96-well test plate. The results (Figure 2B) show that as implemented, the algorithm is remarkably consistent. The concentration of the initial template shows a low coefficient of variation consistent with the manufacturer's thermal stability (±0.4C) across the thermocycler stage.

To assess the efficacy of this approach the application of this technology to three scenarios from our laboratory was examined. These included the confirmation of high-throughput CGH analysis, expression analysis and assessing heterozygosity.

CGH Validation

Fractionation that separates DNA associated with the nuclear matrix from non-associated portions of the genome may now be conducted at the genomic scale and analyzed through both high-throughput sequencing and microarray-based CGH [23]. These technologies provide global snapshots of nuclear architecture. They nonetheless require validation that ensures systematic bias has not been introduced. PCR validation provides an accurate local reference relative to which the high-throughput approaches can be compared and validated. Since unique primers are designed to interrogate DNA in the different fractions, accurate PCR validation requires that reaction efficiencies are appropriately compensated to permit the correct assessment and comparison of relative fractionation.

HeLa cell genomic nuclear matrix and loop associated DNA was fractionated using LIS (lithium 3,5-diiodosalicylate) extraction as described [24]. The loop fraction was labeled with Cy-3 and matrix fraction with Cy-5 respectively then competitively hybridized to high resolution chromosome 16 oligonucleotide arrays (Roche Nimblegen) [23]. Negative signal values on these arrays show DNA to be associated with the nuclear matrix. A series of PCR reactions were designed to amplify 1 kb region of chromosome 16p that by CGH were shown to be consistently associated with the nuclear matrix (Build 36.2 location 589,161 to 590,161). The initial template value for each reaction was calculated using the parametric non-linear fitting model and median values for the replicates were compared. As anticipated the ratio of loop to matrix DNA were reflective of the results obtained with CCH analysis (Table 2).

Expression Analysis

The algorithm described allows the relative expression levels at multiple genic regions to be readily compared even where the primers demonstrate a broad range of amplification

efficiencies. The results permit a rapid quantitative study of the underlying expression trend that does not require a full dilution series for each location.

Expression from each member of the human transgenic PRM1, PRM2 and TNP2 a locus was assessed. Total testis RNA was isolated from transgenic mouse and human tissue. Each gene in the human protamine domain was interrogated using its own primer pair (Tabel 1). Analysis of the relative expression levels of the human protamine genes demonstrated that transgenic animals harboring the human protamine locus expressed the suite of genes (Figure 5) Comparison to the total human testis RNAs demonstrated that expression of the transgene was similar confirming that the transgenic system may act as a functioning model of the human protamine domain (Figure 5).

Zygosity

PCR may allow for the determination of relative copy number and hence the zygosity of transgenic animals without the need for multiplexed PCR reactions or Southern blotting. Though the development of a multiplex PCR assay for such analysis was a significant improvement over the use of radio-labeled probes [25], a more efficient method of ascertaining zygosity was desirable. The non-linear parametric modeling algorithm may be applied to quickly extrapolate the relative template values of a region of DNA. Selection of parallel primer sets directed to a portion of the endogenous genome and the transgenic insertion yields a simple ratio of template values that may be used to establish zygosity.

Following quantification, transgenic DNA was serially diluted and assessed in separate PCR reactions containing primer pairs (Table 1) targeting a portion of the mouse genome or a specific region within a transgenic insertion. The results were analyzed using KLAB-PCR to determine the relative amount of template for each targeted genomic region initially present in the sample. For both primer sets the resulting dose response was correlated ($r^2 = 0.99$; Figure 6). The dilution series is not required but demonstrates the linearity for both primer sets in all samples as determined using this approach. The zygosity of the transgenic animals was then ascertained by comparing the resulting relative amount of template for each amplified regions. Within a single copy transgenic mouse line the inserted region will be present once in a heterozygote and twice in a homozygote. The ratio of the relative template value of the transgenic region to that of the endogenous was 1 for all points in a dilution series in samples isolated from a homozygote (Figure 7A). This ratio is reduced to half in those samples derived from heterozygous individuals (Figure 7B). Similarly, multi-copy transgenic animals are readily identified as the ratio of the relative template value of the transgene to that of the endogenous exceeds 1.

Conclusion

We assume that the maximum efficiency of a reaction may plateau at an E_{max} below 100%. However it is useful to reflect whether this efficiency plateau is constraining in all or only a subset of reactions? The early cycles of a reaction are difficult to observe in any ‘real world’ system. As cycle zero is approached, PCR efficiency may, in some cases, trend asymptotically towards near ideal efficiency. The approach does allow for both a system in which the cycle-zero efficiency is near ideal but quickly departs this level, as well as models with a cycle-zero efficiency of less than 100% that only significantly drops from this level at later cycles (see Figure 1B). The former condition would however benefit from models with additional lower order ($0<n<0.2$) power terms. Future developments will seek to extend this approach.

Acknowledgements

The contributions of Dr Rui Pires Martins to test data generation and his comments on the manuscript are gratefully acknowledged. This work was supported by National Institute of Child Health and Human Development Grant HD36512 (to S.A.K.) and the Department of Obstetrics and Gynecology of Wayne State University (S.A.K.).

References

1. Wang AM, Doyle MV, Mark DF. Quantitation of mRNA by the polymerase chain reaction. Proc Natl Acad Sci U S A 1989;86:9717–9721. [PubMed: 2481313]
2. Roth CM. Quantifying gene expression. Curr Issues Mol Biol 2002;4:93–100. [PubMed: 12074198]
3. Klein D. Quantification using real-time PCR technology: applications and limitations. Trends Mol Med 2002;8:257–260. [PubMed: 12067606]
4. Bustin SA. Quantification of mRNA using real-time reverse transcription PCR (RT-PCR): trends and problems. J Mol Endocrinol 2002;29:23–39. [PubMed: 12200227]
5. Ginzinger DG. Gene quantification using real-time quantitative PCR: an emerging technology hits the mainstream. Exp Hematol 2002;30:503–512. [PubMed: 12063017]
6. Orlando C, Pinzani P, Pazzagli M. Developments in quantitative PCR. Clin Chem Lab Med 1998;36:255–269. [PubMed: 9676381]
7. Gevertz JL, Dunn SM, Roth CM. Mathematical model of real-time PCR kinetics. Biotechnol Bioeng 2005;92:346–355. [PubMed: 16170827]
8. Liu W, Saint DA. Validation of a quantitative method for real time PCR kinetics. Biochem Biophys Res Commun 2002;294:347–353. [PubMed: 12051718]
9. Ostermeier GC, Liu Z, Martins RP, Bharadwaj RR, Ellis J, Draghici S, Krawetz SA. Nuclear matrix association of the human beta-globin locus utilizing a novel approach to quantitative real-time PCR. Nucleic Acids Res 2003;31:3257–3266. [PubMed: 12799453]
10. Tricarico C, Pinzani P, Bianchi S, Paglierani M, Distante V, Pazzagli M, Bustin SA, Orlando C. Quantitative real-time reverse transcription polymerase chain reaction: normalization to rRNA or single housekeeping genes is inappropriate for human tissue biopsies. Anal Biochem 2002;309:293–300. [PubMed: 12413463]
11. Vandesompele J, De Preter K, Pattyn F, Poppe B, Van Roy N, De Paepe A, Speleman F. Accurate normalization of real-time quantitative RT-PCR data by geometric averaging of multiple internal control genes. Genome Biol 2002;3RESEARCH0034
12. Dheda K, Huggett JF, Bustin SA, Johnson MA, Rook G, Zumla A. Validation of housekeeping genes for normalizing RNA expression in real-time PCR. Biotechniques 2004;37:112–114. 116, 118–119. [PubMed: 15283208]
13. Pfaffl MW. A new mathematical model for relative quantification in real-time RT-PCR. Nucleic Acids Res 2001;29:e45. [PubMed: 11328886]
14. Skern R, Frost P, Nilsen F. Relative transcript quantification by quantitative PCR: roughly right or precisely wrong? BMC Mol Biol 2005;6:10. [PubMed: 15854230]
15. Freeman WM, Walker SJ, Vrana KE. Quantitative RT-PCR: pitfalls and potential. Biotechniques 1999;26:112–122. 124–125. [PubMed: 9894600]
16. Rutledge RG, Cote C. Mathematics of quantitative kinetic PCR and the application of standard curves. Nucleic Acids Res 2003;31:e93. [PubMed: 12907745]
17. Ramakers C, Ruijter JM, Deprez RH, Moorman AF. Assumption-free analysis of quantitative real-time polymerase chain reaction (PCR) data. Neurosci Lett 2003;339:62–66. [PubMed: 12618301]
18. Tichopad A, Dilger M, Schwarz G, Pfaffl MW. Standardized determination of real-time PCR efficiency from a single reaction set-up. Nucleic Acids Res 2003;31:e122. [PubMed: 14530455]
19. Rebrikov DV, Trofimov D. Real-time PCR: approaches to data analysis (a review). Prikl Biokhim Mikrobiol 2006;42:520–528. [PubMed: 17066950]
20. Alvarez MJ, Vila-Ortiz GJ, Salibe MC, Podhajcer OL, Pitossi FJ. Model based analysis of real-time PCR data from DNA binding dye protocols. BMC Bioinformatics 2007;8:85. [PubMed: 17349040]
21. Peirson SN, Butler JN, Foster RG. Experimental validation of novel and conventional approaches to quantitative real-time PCR data analysis. Nucleic Acids Res 2003;31:e73. [PubMed: 12853650]

22. Goodrich RJ, Ostermeier GC, Krawetz SA. Multitasking with molecular dynamics Typhoon: quantifying nucleic acids and autoradiographs. Biotechnol Lett 2003;25:1061–1065. [PubMed: 12889815]

23. Linnemann AK, Platts AE, Doggett N, Gluch A, Bode J, Krawetz SA. Genomewide identification of nuclear matrix attachment regions: an analysis of methods. Biochem Soc Trans 2007;35:612–617. [PubMed: 17511663]

24. Kay, V.; Bode, J. Detection of scaffold-attached regions (SARs) by in vitro techniques; activities of these elements in vivo. In: Papavassiliou, AG.; King, SL., editors. Methods in Molecular and Cellular Biology: Methods for studying DNA-protein interactions - an overview. Wiley-Liss; 1995. p. 186-194.

25. Martins RP, Krawetz SA. Using multiplexed real-time polymerase chain reaction to rapidly identify single-copy transgenic animals. Anal Biochem 2004;329:337–339. [PubMed: 15158496]

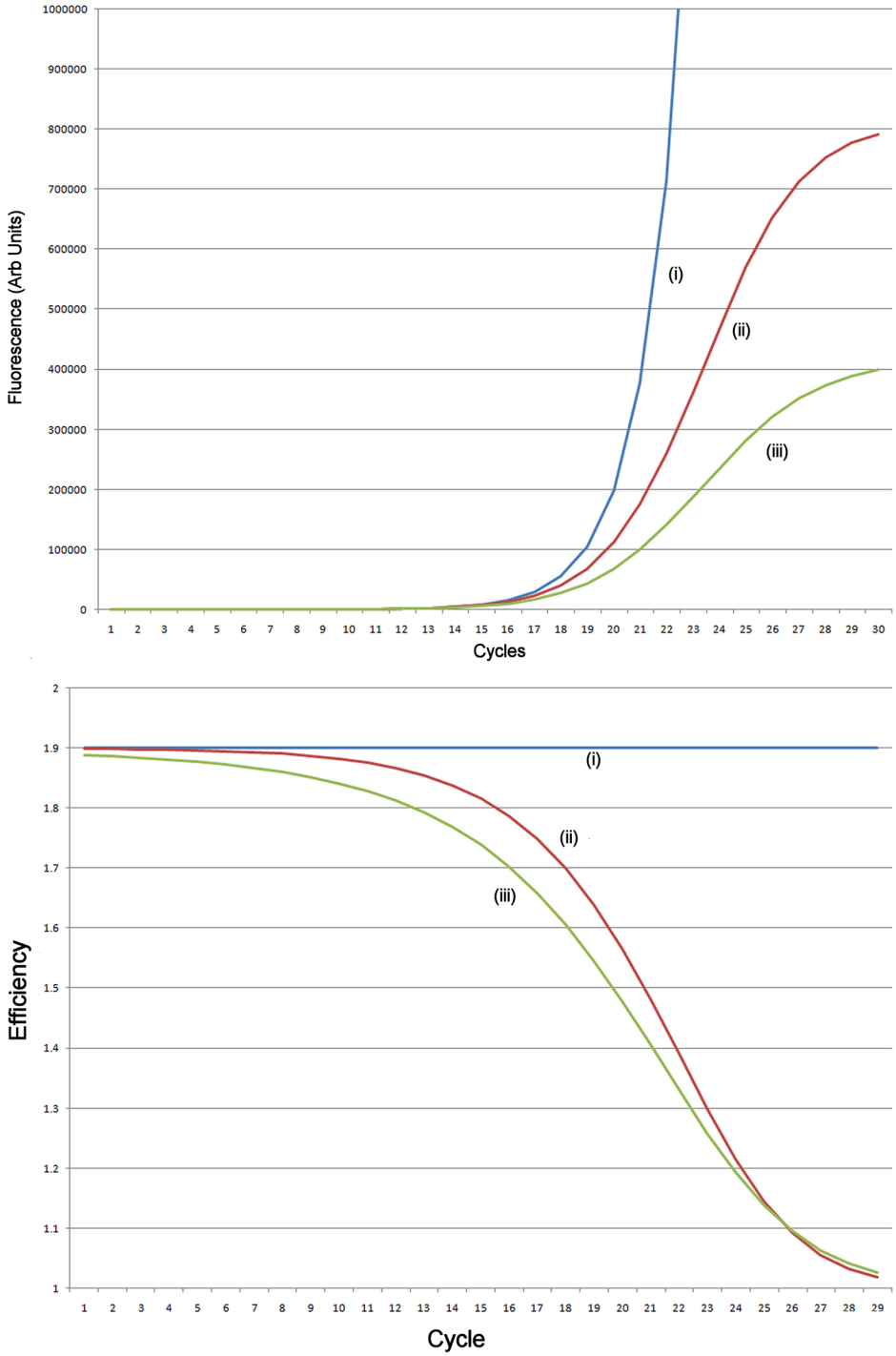

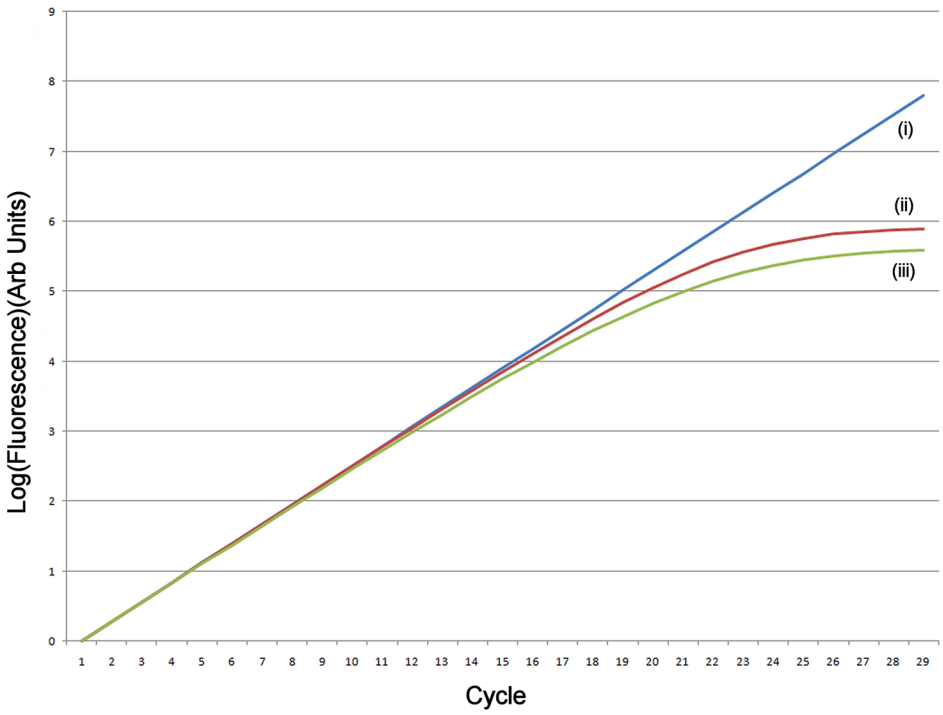

Figure 1.

Simulation of amplification. (A) A simulated exponential amplification curve with E_{max}=1.9 (*i*) generated using an unconstrained efficiency $T_{n+1}=T_n \times 1.9$ (T_0=1), (*ii*) efficiency limited as a simple function of increasing template $T_{n+1}=T_n \times (1.9-0.001\times T_n^{0.5})$, and (*iii*) efficiency limited by a more physically realistic function $T_{n+1}=T_n \times (1.9-(0.001\times T_n^{0.5} + 0.01\times T_n^{0.25}))$. (B) Reaction efficiency as a function of cycle for the three models. (C) Log (fluorescence) of the exponential amplification.

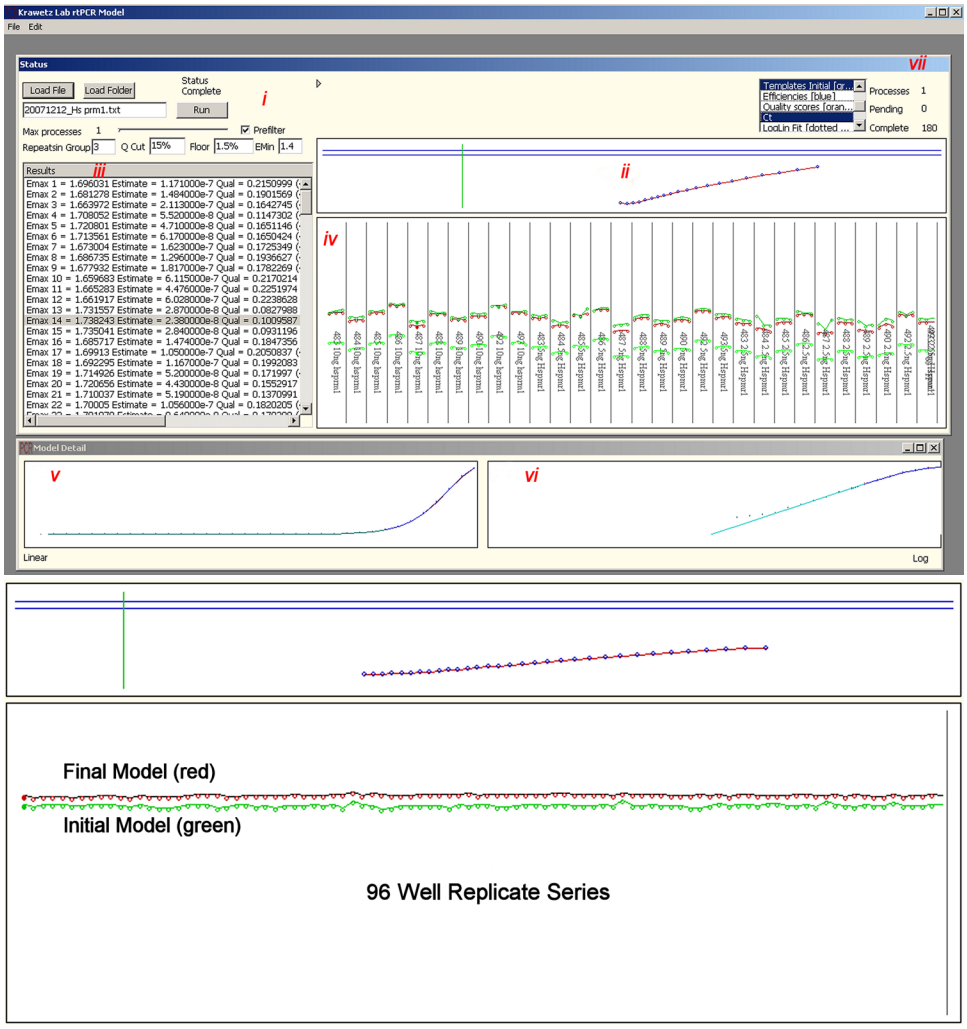

Figure 2.

The user interface of KLAB-PCR. The window driven interface includes (*i*) data loading and analysis preferences (*ii*) E(max) identification through the first non-linear model (*iii*) data output including E_{max}, template estimation and model quality (*iv*) a graphical representation of template estimates from the first model (top green) final model (middle red) and C_t approaches (lower green) (*v*) PCR amplification curve (blue) generated from the final model and data curve (red) (*vi*) Log-linear fit (blue) to data (red) (*vii*) Progress of analysis. Replicates may be grouped based on sets of primers (A) or treated as a single group for example where the same reaction is replicated across 96 wells (B).

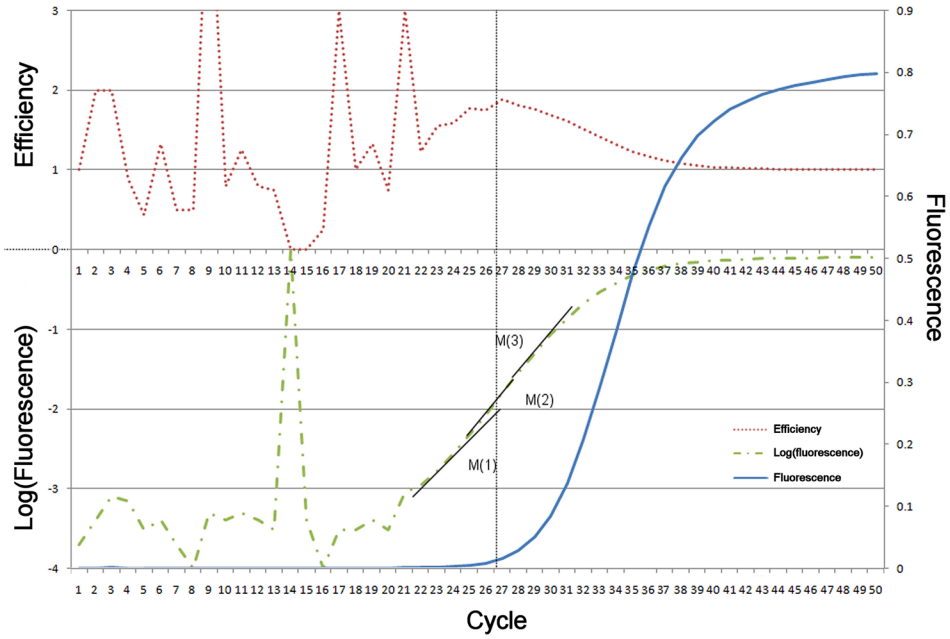

Figure 3.

PCR fluorescence data (blue – right axis) measured on a Chromo4 Thermocycler, together with efficiency (red – left axis) and log(fluorescence) (green – left axis). Three tangents M(1–3) are shown relative to the log signal. M(1) demonstrates the highest local linearity (R^2=0.9993) but is in the poorly resolved low-signal segment. The range of initial template predicted by M(1–3) varies from 1.5e-2 to 2e-3 demonstrating the sensitivity to data selection.

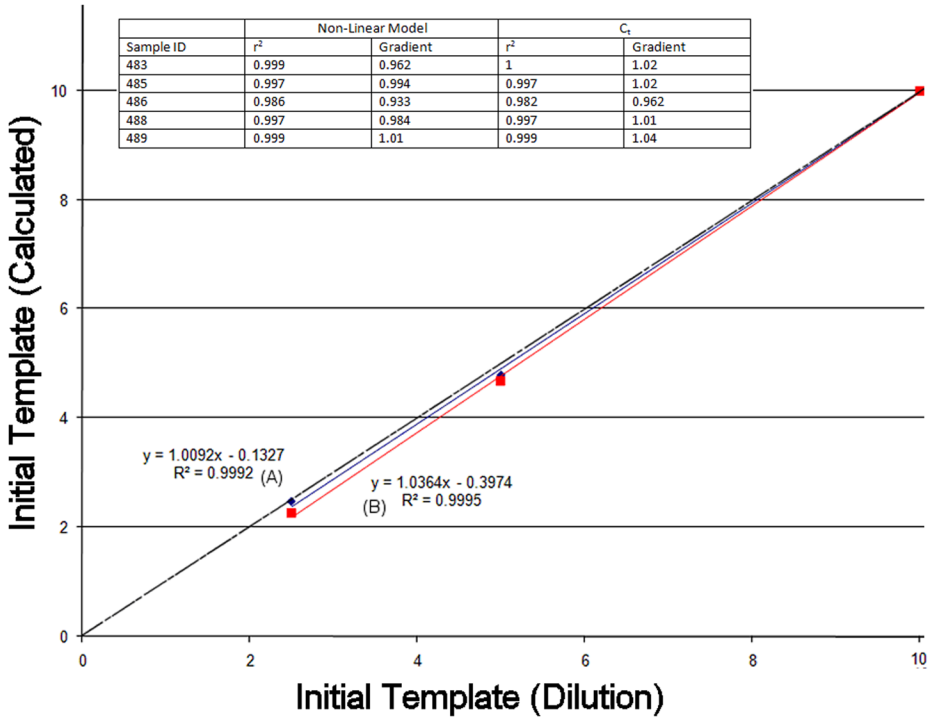

Figure 4.

Genomic template concentration calculated using the known dilution (X) and also by the two approaches described (Y). Initial template (Protamine 1, primers Table 1) (10 units) was serially diluted by a factor of 2 and 4 and reactions undertaken on a Chromo4 thermocycler. The non-linear model (A, blue) and C_t model (B, red) both closely parallel each other in this reaction due to the near perfect reaction efficiency. The r^2 and gradients for five different biological samples are also shown (inset table). Ideal values for the gradients and r^2 values are 1 as indicated by the dotted line in the chart.

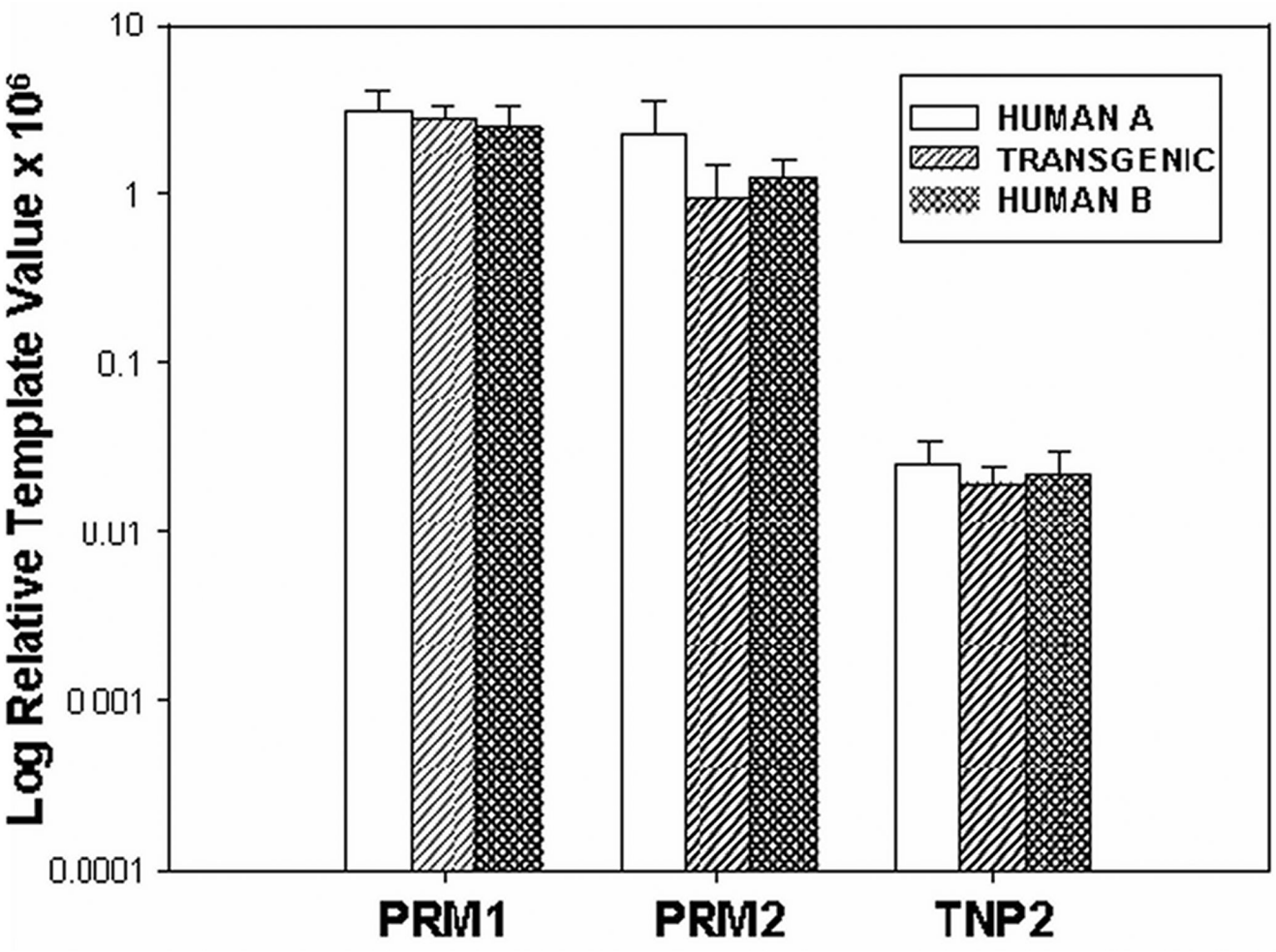

Figure 5.
Relative level of expression of the members of the human protamine locus. The expression of human PRM1, PRM2, and TNP2 genes were assayed by qRT-PCR of total testis RNA. Relative expression was determined by the parametric modeling approach. Expression of the suite of genes in transgenic animals was similar to that observed in human.

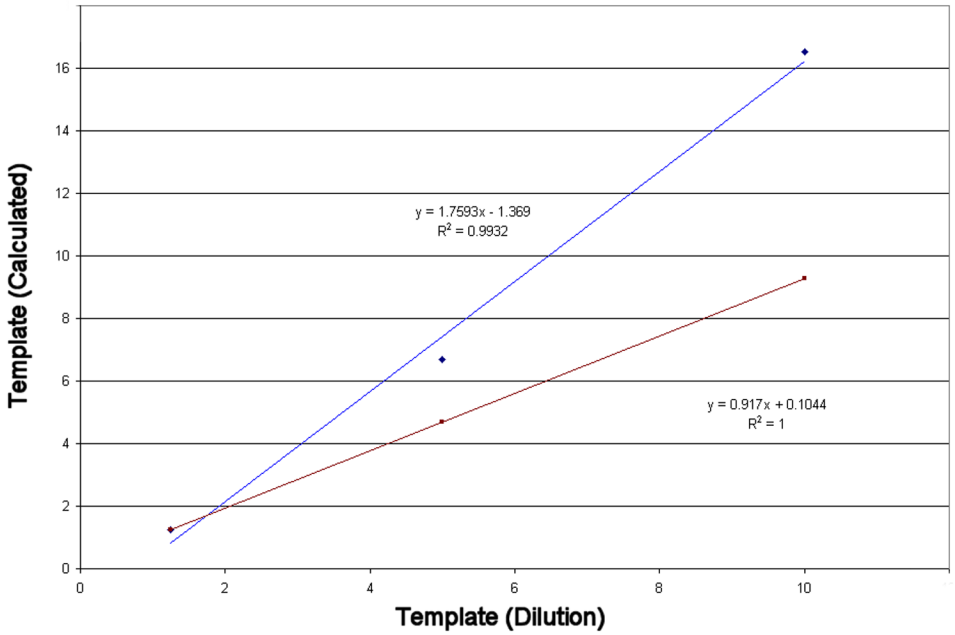

Figure 6.

Performance of the non-linear and C_t models. The reaction efficiency was not-ideal (E_{max}=1.75). While both approaches exhibit a linear response as a function of the template concentration, the C_t approach significantly over-estimates the dilution rate where the model generally reflects the dilution series.

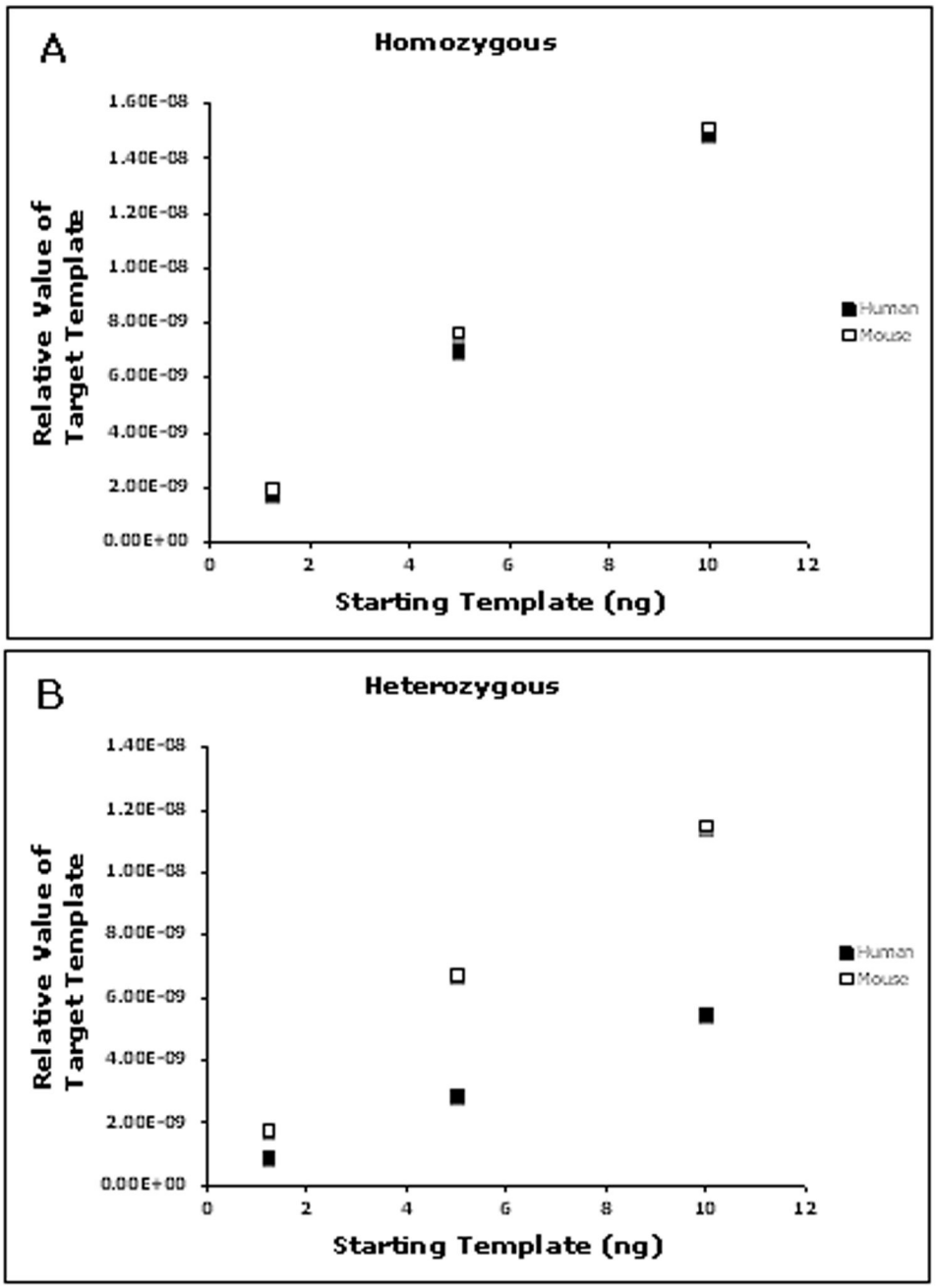

Figure 7.

Determination of zygosity by comparison of transgene and endogenous template values. Serially diluted DNA isolated from single copy transgenic mice was subjected to PCR analysis with primer pairs Determination of Copy number. An endogenous region of the genome or a portion of the human transgene were targeted for PCR analysis. Data from separate reactions was combined to demonstrate the different ratios of relative template values of the templates indicative of a homozygous (A) or heterozygous (B) state.

Table 1

Primers used for the determination of copy number, CGH and relative expression.

PRIMER NAME	FORWARD (5' – 3')	REVERSE (5' – 3')	AMPLICON SIZE	T_a
CGH VALIDATION PRIMERS				
Human Chromosome 16:589541 – 590150	CGTGGGTGTTCGCTACTGT	AGAGGCTCCAACATCAAGGG	609	**65**
EXPRESSION ANALYSIS PRIMERS				
PRM1*	CGGAGCTGCCAGACACGGA	CTACATCTCGGTCTGTACCTGGG	65	64
PRM2*	AAGACGCTCCTGCAGGCAC	GCCTTCTGCATGTTCTCTT	71	64
TNP2	GCCTTCTGCATGTTCTCTT	TTGCGTAGAAATCACCATAGT	1161	64
ZYGOSITY PRIMERS				
Mouse Chromosome 1610802607:10802980	TTAAAGATAATGCGGGATGTAT	GCTCCAAGGCAACTCTTAAT	373	52
PRM1	CAGAGCCGGAGCAGATATTACC	ATTTATTGACAGGCGGCATTGTT	359	62.5

*Steger K, Wilhelm J, Konrad L, Stalf T, Greb R, Diemer T, Kliesch S, Bergmann M, Weidner W. Both protamine-1 to protamine-2 mRNA ratio and Bcl2 mRNA content in testicular spermatids and ejaculated spermatozoa discriminate between fertile and infertile men. Human Reproduction 2008 23 (1):11–16

Table 2

Loop/Matrix Genome Fractionation. (A) Initial template values from triplicate amplifications of loop and matrix DNA were calculated using the KLab PCR parametric modeling. Ratios of loop:matrix median values were used to determine the percentage of the total DNA in each fraction. (B) CGH array analysis of the fractionated genomic DNA probed within the amplified region.

A.

Region Amplified	Reaction Name	Initial Template	Median Values	% of Total
589,161 – 590,161	HeLa LIS Loop 1	1.36E-05	0.0000175	38%
	HeLa LIS Loop 2	1.75E-05		
	HeLa LIS Loop 3	2.12E-05		
	HeLa LIS Matrix 1	2.86E-05	0.0000286	62%
	HeLa LIS Matrix 2	2.96E-05		
	HeLa LIS Matrix 3	2.37E-05		

B.

Chromosome 16 Genomic Probe Location	Normalized Matrix Percentage
589,501	60%
590,181	66%